

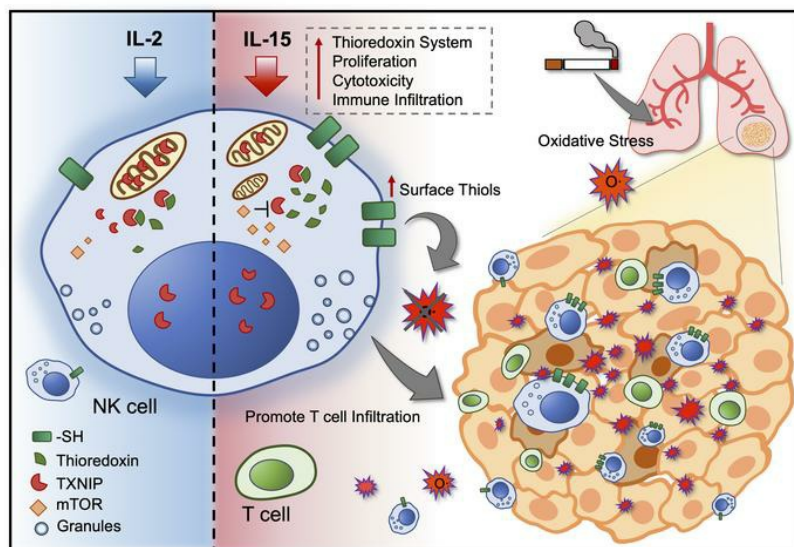
Thioredoxin activity confers resistance against oxidative stress in tumor-infiltrating NK cells

Ying Yang, ... , Kai Wang, Andreas Lundqvist

J Clin Invest. 2020. <https://doi.org/10.1172/JCI137585>.

Research In-Press Preview Immunology Oncology

Graphical abstract



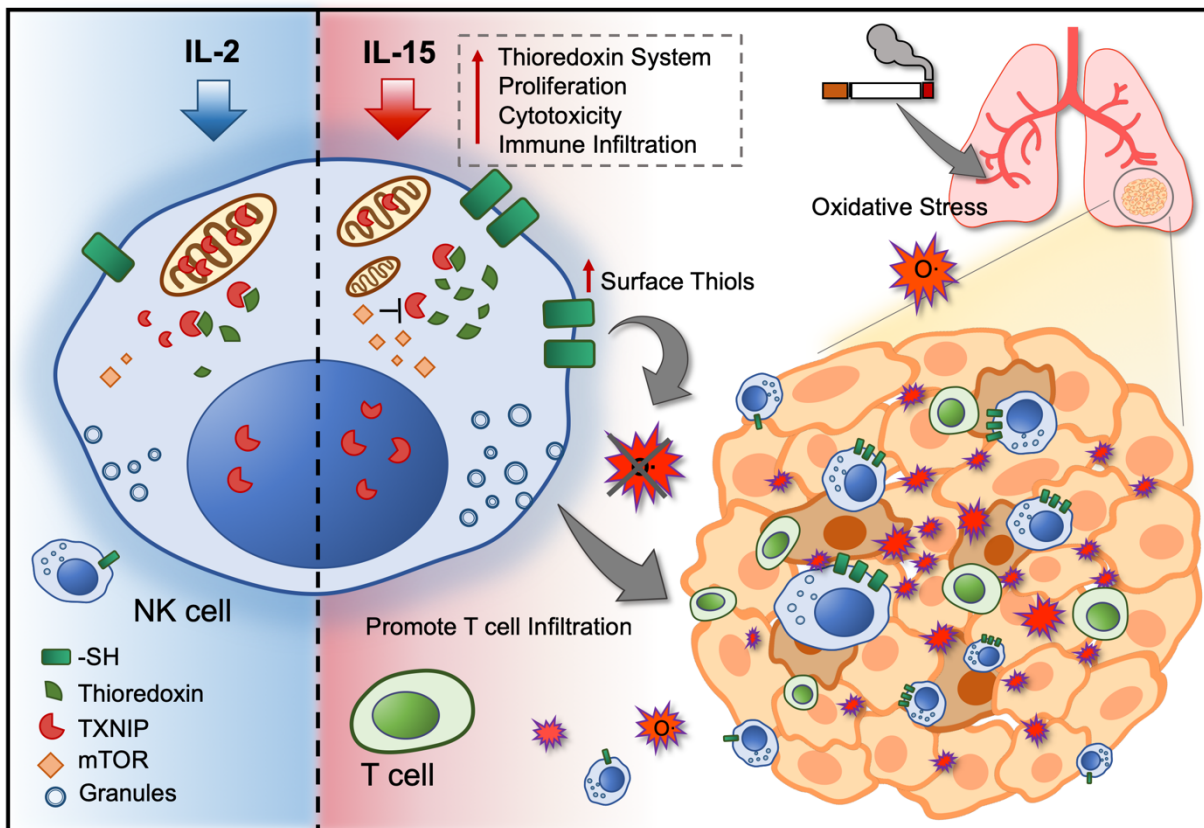
Find the latest version:

<https://jci.me/137585/pdf>



28 **Abstract**

29 To improve the clinical outcome of adoptive NK cell therapy in patients with solid tumors,
30 NK cells need to persist within the tumor microenvironment (TME) in which the abundance
31 of reactive oxygen species (ROS) could dampen anti-tumor immune responses. In the
32 present study, we demonstrated that IL-15 primed NK cells acquire resistance against
33 oxidative stress through thioredoxin system activated by mTOR. Mechanistically, the
34 activation of thioredoxin showed dependence on localization of thioredoxin-interacting
35 protein. For the first time, we show that NK cells residing in the tumor core expressed
36 higher thiol density which could aid to protect other lymphocytes against ROS within the
37 TME. Furthermore, the prognostic value of *IL15* and NK cell gene signature in tumors
38 may be influenced by tobacco smoking history in NSCLC patients. Collectively, the levels
39 of reducing antioxidants in NK cells may not only predict for better tumor penetrance but
40 even potentially response to immune therapy.



43 **Introduction**

44 Reactive oxygen species (ROS) are a diverse class of radical species that have different
45 roles depending on their concentration. Considering their immune suppressive effects,
46 ROS have been proposed as metabolic immune checkpoint within the tumor
47 microenvironment (TME) (1-3). ROS is produced not only by stressed and highly
48 metabolic tumor cells but also by activated immune cells such as granulocytes,
49 macrophages and myeloid-derived suppressor cells. While oxidative stress is a double-
50 edged sword in cancer biology, targeting the antioxidant pathway may represent be a
51 good strategy to be used in combination with immunotherapy (4). Antioxidants such as
52 reducing enzymes provide tumor cells with resistance against high oxidative stress but
53 on the contrary, the TME may potentially be reshaped with increasing immune infiltration
54 and persistence of cytotoxic lymphocytes (5, 6). Thioredoxin is one of the main
55 antioxidants in the cellular redox system which functions as a scavenger for ROS with its
56 primary function to reduce oxidized cysteine residues and cleave disulfide bonds (7, 8).
57 Elevated levels of thioredoxin often correlate with immune activation, regulating the
58 survival of immune cells (9-11).

59 Since tobacco smoking is one of the major cause of lung cancer and contributes to the
60 accumulation of oxidative stress in the lung TME (12, 13), lung cancer represents one of
61 the more relevant cancer types to study the impact of ROS on immunity (4). Tobacco
62 smoking by itself not only contains high concentrations of ROS but also triggers
63 inflammation, activating immune cells to upregulate ROS production (14). However,
64 tobacco smoking may implicate the survival of lymphocytes residing in the lungs and
65 hence, modulating the tissue's immune landscape. A hallmark study also highlighted that

66 smoking signature influences tumor mutational burden and sensitivity to PD-1 blockade
67 in NSCLC (15). The patients' smoking history may indeed influence clinical response to
68 immune therapy even though the dogma still remains that tobacco smoking promotes
69 lung cancer progression.

70 Natural Killer cells are cytotoxic lymphocytes that contributes to immune surveillance
71 against viral infections and cancer. Unlike conventional CD8 T cells, the cytotoxicity
72 functions of NK cells are robustly regulated by a repertoire of activating and inhibitory
73 receptors. One of the key inhibitory ligands to provide a "don't kill" signal is major
74 histocompatibility complex (MHC) class I, which is often downregulated, resulting in
75 increased sensitivity to NK cell-mediated cytotoxicity within the tumor (16-18). Existing
76 therapeutic approaches to harness NK cells for cancer immunotherapy include adoptive
77 cell therapy and inhibitors against NK cell checkpoints. However, adoptive NK cell therapy
78 so far has been only beneficial against hematological cancers given its poor penetrance
79 into solid tumors and inadequate cytotoxicity against tumor cells (19). Moreover, the
80 function and fate of these NK cells are highly prone to be influenced by the highly dynamic
81 TME, not forgetting that tissue-infiltrating NK cells may not be merely "killers" but undergo
82 phenotypic switch to acquire other non-canonical functions (20-22).

83 Our previous study demonstrated that modulating NK cells with IL-15 for adoptive cell
84 therapy enhances effector functions regulated by STAT5 signaling and mTOR activation
85 (23). Knowing that oxidative stress have profound immune suppressive effects on NK
86 cells (1-3), the present study sought to investigate if IL-15 and mTOR activation of NK
87 cells may confer resistance against oxidative stress. For the first time, we show how
88 thioredoxin activity regulates thiol density expressed on membrane surface of NK cells

89 serving as a reducing shield that also protects neighboring T cells against oxidative stress.
90 With a particular interest to study non-small cell lung cancer, we uncovered that NK cells
91 within the tumor core showed higher surface thiol densities as compared to NK cells found
92 in the tumor periphery and adjacent normal lung tissues. The accumulation of intracellular
93 ROS in NK cells was also found to be higher in tumor periphery and normal tissues of
94 NSCLC patients with history of tobacco smoking. From TCGA public database, we
95 observed the prognostic value of NK cell gene signature and *IL15* gene expression in the
96 tumor could be influenced by the tobacco smoking history of the patients.

97

98 **Results**

99 **IL-15 primed NK cells mount superior immune response under oxidative stress.**

100 To test whether IL-2 and IL-15 differ in their ability to render NK cells less susceptible to
101 oxidative stress, the activity of cytokine-primed NK cells was analyzed following exposure
102 to H₂O₂ treatment. At lower effector to target ratio, IL-15 primed NK cells showed greater
103 ability to kill K562 target cells compared with IL-2 primed NK cells (Figure 1A). With
104 exposure to H₂O₂ at a dose of 5μM and at an effector to target ratio of 9:1, the ability of
105 both IL-2 and IL-15 primed NK cells to kill K562 target was not reduced compared with
106 control cell not exposed to H₂O₂. However, at a lower effector to target ratio of 3:1, the
107 cytotoxicity by IL-2-primed NK cells was significantly reduced compared with IL-15-primed
108 NK cells. Regardless of effector to target ratios, cytotoxicity by both IL-2 and IL-15 primed
109 NK cells were significantly reduced when exposed to a higher H₂O₂ dose of 10μM. Still,
110 the ability of IL-15 primed NK cells to kill K562 target cells was significantly higher
111 compared with IL-2 primed NK cells (Figure 1B). Similarly, in response to K562 stimulation,
112 IL-15 primed NK cells showed significantly higher degranulation and production of IFN-γ
113 compared with IL-2 primed NK cells. In the presence of high dose H₂O₂ of 10μM, IL-15
114 primed NK cells showed significantly higher degranulation and production of IFN-γ
115 compared with IL-2 primed NK cells (Figure 1C and D). While intracellular ROS is known
116 to be immune suppressive to NK cells, the levels of intracellular ROS was analyzed in
117 cytokine-primed NK cells. These experiments revealed that IL-15 primed NK cells have a
118 reduced accumulation of intracellular ROS compared with IL-2 primed NK cells at the
119 same doses of H₂O₂ (Figure 1E and F). Both concentrations of H₂O₂ treatment did not
120 significantly affect the viability of IL-2 or IL-15 primed NK cells. In terms of cell proliferation,

121 IL-15 primed NK cells were equally susceptible to H₂O₂-mediated suppression compared
122 to IL-2 primed NK cells (data not shown). From these observations, we hypothesized that
123 IL-15 primed cells could intrinsically acquire functions to eradicate ROS from an H₂O₂ rich
124 environment and hence maintain their functional activity to kill target cells and produce
125 IFN- γ .

126

127 **IL-15 upregulates thioredoxin activity in NK cells by both gene expression and**
128 **reduced shuttling of mitochondrial TXNIP.**

129 To investigate the underlying mechanisms for the increased resistance to oxidative stress
130 by IL-15 primed NK cells, transcriptomic analysis of publicly available sequencing data
131 was performed (23). Through gene enrichment analysis, amongst the top enriched gene
132 ontologies (Supplementary Figure 1A) were genes related to oxidoreductase activity
133 (Supplementary Figure 1B). In analyzing genes related to response to ROS, elevated
134 gene expression of thioredoxins (*TXN* and *TXN2*) and reduced expression of their
135 inhibitory counterparts (*TXNIP* and *TXNRD1*) were identified (Figure 2A and
136 Supplementary Figure 1C to F). At the protein level, IL-15 primed cells expressed higher
137 level of thioredoxin-1 (Figure 2B). However, no significant differences of TXNIP protein
138 expression was observed by flow cytometry analysis between IL-2 and IL-15 primed NK
139 cells (data not shown). In contrast, differences in subcellular localization of TXNIP was
140 observed. Exposure to H₂O₂ induced the release of TXNIP from the nucleus (Figure 2C),
141 and the expression of TXNIP was significantly higher within the nucleus of IL-15 primed
142 NK cells compared with IL-2 primed NK cells (Figure 2D). Furthermore, exposure to H₂O₂
143 of IL-2 but not IL-15 primed NK cells resulted in shuttling of TXNIP into the mitochondria

144 in where thioredoxin-2 is expressed (Figure 2E). The beneficial roles of IL-15 in the
145 current context could be explained by the downregulation of CD25 (IL-2 receptor alpha)
146 and the upregulation of CD215 (IL-15 receptor alpha) upon exposure to H₂O₂
147 (Supplementary Figure 1G and H). The common receptor subunit of both IL-2 and IL-15
148 signaling, CD122 (IL-2 receptor beta) remained unchanged under oxidative stress
149 (Supplementary Figure 1I). These changes in subcellular localization and expression
150 profiles provide an understanding how thioredoxin activity is regulated in NK cells to
151 reduce intracellular ROS for improved immune functions by IL-15 primed NK cells.

152

153 **NK cells express high surface thiol density to serve as a reducing shield against**
154 **ROS to sustain cytotoxicity function.**

155 In addition to the thioredoxin system that reduces intracellular ROS, cell surface thiols
156 can act as a protective shield as they get oxidized by external free radicals. Using
157 maleimide that binds to protein thiols without interfering with their function, IL-15 primed
158 NK cells showed significantly higher levels of cell surface thiols compared with IL-2 primed
159 NK cells (Figure 3A). Following exposure to H₂O₂, both IL-2 and IL-15 primed NK cells
160 showed reduced expression of cell surface thiol density (Figure 3B). Moreover, only NK
161 cells with low thiol density (low maleimide fluorescence intensity) showed an
162 accumulation of intracellular ROS after H₂O₂ treatment (Figure 3C). Regardless of
163 stimulation with IL-2 or IL-15, NK cells with high surface thiol density (FACS-sorted based
164 on maleimide fluorescence intensity) showed superior killing of K562 target cells in the
165 presence of H₂O₂ (Figure 3D). In analyzing regulation of thioredoxin and NK cell
166 phenotype, NK cells with high surface thiol density also expressed higher levels of CD56,

167 CD16, and thioredoxin. These NK cells also displayed increased mTOR activation as
168 measured by the phosphorylation of S6 kinase (Figure 3E). In terms of subcellular location,
169 TXNIP was enriched in the cytoplasm in NK cells with lower thiol density (Figure 3F).
170 These results indicated that surface thiol density in NK cells is associated with favorable
171 anti-tumor functions and resistance against ROS-mediated immune suppression.

172

173 **Inhibition of thioredoxin-1 reduces NK cell surface thiol density and reverses IL-15**
174 **mediated resistance against oxidative stress.**

175 Since thioredoxins and surface thiols are expressed at higher levels in IL-15 primed NK
176 cells, we sought to investigate if the thioredoxin system plays a role in the regulation of
177 surface thiols and to validate that thioredoxin-1 has an important role in conferring
178 resistance to ROS-mediated immune suppression. In the presence of the selective
179 thioredoxin-1 inhibitor PX-12, surface thiols were significantly reduced in both IL-2 and
180 IL-15 primed NK cells (Figure 4A). Additionally, under PX-12 inhibition, surface thiols of
181 both IL-2 or IL-15 primed NK cells exhibited less reduction in the presence of H₂O₂
182 (Supplementary Figure 2A). Upon PX-12 treatment, similar levels of accumulated ROS
183 were observed in both IL-2 and IL-15 primed NK cells (Figure 4B). In addition, the
184 presence of PX-12 abrogated the ability of IL-15 primed NK cells to kill K562 cells upon
185 exposure to H₂O₂ (Supplementary Figure 2B). Using a physiological model of oxidative
186 stress, NK cells were cultured with autologous activated neutrophils. In these experiments,
187 PX-12 treatment resulted in higher intracellular ROS levels in IL-15 treated cells (Figure
188 4C). Moreover, ROS produced by the activated neutrophils suppressed the proliferation

189 of NK cells and treatment with PX-12 reduced the proliferation of IL-15 primed NK cells
190 to the same levels of untreated IL-2 primed NK cells (Figure 4D).

191 To determine whether NK cells could be affected by ROS produced by tumor cells, a lung
192 adenocarcinoma 3D sphere model was used (Supplementary Figure 2C). NK cells that
193 infiltrated and localized inside the sphere were found to accumulate more intracellular
194 ROS (Supplementary Figure 2D). Inhibition of thioredoxin-1 resulted in significant
195 reduction in infiltration by IL-15 primed NK cells (Figure 4E and F). Furthermore, purified
196 NK cells with high surface thiol density showed superior ability to infiltrate lung tumor
197 spheres (Figure 4G). The removal of surface thiols by N-ethylmaleimide in IL-15 primed
198 NK cells also resulted in reduced infiltration into tumor spheres (Supplementary Figure
199 2E and 2F). In contrast, the addition of exogenous thioredoxin-1 instead promoted the
200 infiltration of IL-2 primed NK cells into the tumor spheres (Supplementary Figure 2G).
201 Taken together, there is a causal relationship between thioredoxin-1 expression and the
202 surface thiol density by NK cells. In two separate physiological models of ROS, IL-15-
203 primed NK cells show increased ability to resist ROS-mediated immune suppression.

204

205 **mTOR activation suppress the expression of TXNIP to sustain thioredoxin activity**
206 **and cell surface thiol density.**

207 We previously identified mTOR activation as an important difference to discriminate
208 functional outcomes between IL-15 and IL-2 primed NK cells (23). To investigate if mTOR
209 activation was linked to the expression of thioredoxin (Trx), thioredoxin interacting protein
210 (TXNIP) and cell surface thiol density, the selective mTOR inhibitor Torin-1 was added to
211 cytokine-primed NK cells. Indeed, the presence of Torin-1 resulted in upregulation of

212 TXNIP in IL-15 primed NK cells (Figure 5A). Upon Torin-1 treatment, a reduction in Trx
213 activity was observed (Figure 5B). Notably, the difference of thioredoxin expression
214 between IL-2 and IL-15 NK cells diminished upon treatment with Torin-1 (Figure 5C).
215 Similarly, there were also no significant differences in cell surface thiol density or
216 accumulation of intracellular ROS between IL-2 and IL-15 primed NK cells upon treatment
217 with Torin-1 (Figure 5D and E). The addition of the mTOR agonist MHY1485 also
218 increased cell surface thiol density and reduced the accumulation of intracellular ROS in
219 NK cells (data not shown). Treatment with Torin-1 also resulted in the shuttling of TXNIP
220 out of the nucleus in IL-15 primed NK cells (Figure 5F-H). These findings demonstrated
221 that mTOR is a key regulator of thioredoxin system and hence, for the IL-15 mediated
222 resistance against oxidative stress.

223

224 **NK cell infiltration is influenced by the accumulation of oxidative stress in NSCLC** 225 **tumors**

226 From a cohort of NSCLC patients (Supplementary Table 1), a higher frequency of CD56
227 positive lymphocytes within tissue sections obtained from tumor periphery as compared
228 to the tumor core was observed (Figure 6A). In a more detailed analysis where samples
229 were segregated into the different tissue locations; tumor core, tumor periphery, and
230 adjacent normal lung tissue (Supplementary Figure 3A), significantly higher frequencies
231 of NK cells in the peripheral tumor region and normal adjacent tissue compared to the
232 tumor core were observed (Figure 6B). NK cells within the tumor core showed significantly
233 higher intracellular ROS level compared with NK cells residing in the tumor periphery and
234 adjacent normal tissues (Figure 6C). In addition, there was a significant negative

235 correlation between levels of intracellular ROS and the frequency of tissue-infiltrating NK
236 cells (Figure 6D). Segregating the data obtained from different tissue regions, a significant
237 and strong negative correlation was observed in normal tissue and the tumor periphery
238 but not for the tumor core (Figure 6E-G). Given that these tissues in general displayed
239 high positivity for 8-OHdG expression (Supplementary Figure 3B), oxidative stress had
240 significant implications on NK cell infiltration and the accumulation of intracellular ROS
241 within NSCLC tumors.

242

243 **NK cell signature and *IL15* gene expression predict better prognosis in NSCLC**
244 **patients with a smoking history**

245 In analyzing of TCGA data, the gene expression of *IL15* from bulk tumor sequencing
246 positively correlated with several NK cell gene signature scores within the NSCLC cohort
247 (Supplementary Figure 3C). To confirm our results on the association of NK cell infiltration
248 and oxidative stress, analysis of TCGA data was performed. Since tobacco smoking is
249 known to induce tissue ROS production, the TCGA-LUAD dataset were segregated into
250 a smoker and a non-smoker cohort (Supplementary Figure 3D). Using a set of oxidative
251 stress-related genes that were found to correlate with worse prognosis in lung cancer (24),
252 smokers showed a higher score of oxidative stress gene signature (Supplementary Figure
253 3E). Even though neither NK cell signature nor *IL15* gene expression alone correlated
254 with better prognosis in the NSCLC cohort (data not shown), the prognostic values of NK
255 cell signature and *IL15* gene expression was influenced by patient's smoking history.
256 Remarkably, NK cell gene signature predicted overall survival (OS) and progression free
257 interval (PFI) only in the smoker cohort (Figure 7A and B) whereas no significant

258 observation was seen in the non-smoker group (Supplementary Figure 3F and G).
259 Similarly, *IL15* gene expression was only predictive for PFI in the smoker cohort (Figure
260 7C and Supplementary Figure 3H). From our NSCLC patient cohort in which FACS
261 phenotyping was performed, a significantly higher level of intracellular ROS in NK cells
262 residing in tumor periphery and adjacent normal lung tissue of smokers was observed
263 (Figure 7D). Notably, this trend in ROS accumulation was not observed in the context of
264 tissue-infiltrating T cells (Figure 7E).

265

266 **High surface thiol density on tumor-infiltrating NK cells improve immune**
267 **infiltration into tumors**

268 To validate that high surface thiol density on NK cells would improve infiltration into tumors,
269 the expression of surface thiols on NK cells residing in the tumor core, periphery and
270 adjacent normal tissues surgically resected from NSCLC patients were analyzed. NK cells
271 within the tumor core expressed the highest surface thiol densities as compared to those
272 in tumor periphery and normal tissue (Figure 8A and B). From a previously published
273 NSCLC tumors and peripheral blood dataset, we observed larger proportions of CD45-
274 positive TILs including CD8 T cells and NK cells to have a higher enrichment for pathways
275 related to oxidoreductase and thioredoxin disulfide reductase activities as compared to
276 cells from peripheral blood (Figure 8C). Focusing on the NK cell population, the
277 normalised enrichment scores for these 2 gene ontology (GO) pathways were higher in
278 tumor-infiltrating NK cells than peripheral blood NK cells (Supplementary Figure 4A and
279 4B). Pooling NK cell data from both blood and tumor samples, we also observed that cells
280 enriched for either of these 2 GO pathways also had higher cytotoxicity gene set scores

281 (Supplementary Figure 4C and 4D). While high thioredoxin activity was associated with
282 enhanced cytotoxicity functions, purified NK cells with high and low surface thiol density
283 were tested for their ability to protect neighboring TILs from ROS-mediated immune
284 suppression in a bystander fashion. Using autologous patient derived tumor spheres,
285 improved autologous TILs infiltration as observed upon addition of NK cells sorted for
286 high thiol density compared with the addition of NK cells sorted for low thiol density (Figure.
287 8D and E). Through the expansion of TILs from patients with NSCLC and sarcoma
288 (Supplementary Table 2), IL-15 expanded a higher frequency of TIL-NK cells with higher
289 surface thiol density (Figure 8F). From these TILs cultures, we observed that there was
290 only a significant increase in the frequency of NK cells and dividing NK cells in IL-2
291 cultures treated with the ROS scavenger catalase (Supplementary Figure 4E and F).

292 **Discussion**

293 ROS can be produced by several cell types within the tumor microenvironment and
294 accumulate along with tumor progression. It is well established that NK cells are
295 susceptible to ROS-mediated immune suppression. Often, myeloid cells within the TME
296 produce high levels of ROS to inhibit the anti-tumor functions of NK cells which has
297 implications for tumor progression and the formation of distant metastasis (1-3). In
298 addition, clinically approved antibodies such as rituximab can trigger ROS production by
299 myeloid cells, suggesting oxidative stress as a means of resistance against NK cell-
300 dependent therapies (25). Here we compared the ability of the two type cytokines, IL-2
301 and IL-15, to modulate the response of NK cells to ROS and found that IL-15 render NK
302 cells less susceptible to oxidative stress through increased thioredoxin system within
303 tumor microenvironment.

304 The expression of thioredoxin is commonly associated with TCR signaling and immune
305 activation (10, 26-28). Early studies showed that thioredoxin activation is a sign of
306 inflammation and is chemotactic to multiple immune cells (29). Yet, the current
307 understanding of thioredoxin pathway in immune cells, particularly NK cells, is not fully
308 understood. We observed that CD56^{bright} subset of NK cells expressed higher levels of
309 thioredoxin and persistence in lung tumors (data not shown). This could further explain
310 how IL-15 agonist (ALT-803) priming enhances anti-tumor responses by CD56^{bright} subset
311 of NK cells isolated from multiple myeloma patients (30). Another recent study showed
312 that the expansion of NK cells with K562 expressing 4-1BBL and membrane IL-15
313 upregulates the expression of thioredoxin and peroxiredoxin which act as antioxidants
314 conferring NK cells resistant against H₂O₂-mediated oxidative stress (31). Apart from

315 expression levels of Thioredoxin and inhibitory counterpart, TXNIP, we showed in NK
316 cells that the subcellular localization and shuttling of TXNIP has a crucial role in regulation
317 of thioredoxin activity. As previously also shown in pancreatic beta cells, the shuttling of
318 TXNIP from the nucleus to the mitochondria within the cell is a response to oxidative
319 stress. This in turn leads to ASK1 phosphorylation and cell death (32). In the immunology
320 context, the thioredoxin-ASK1 axis was also found to regulate the selection and survival
321 of double positive thymocytes during T cell development (9). While our previous study on
322 the effects of IL-15 on NK cells revealed that mTOR activation acts as a main driver for
323 enhanced immune functions, it could be plausible that mTOR activation could be a
324 regulator for thioredoxin system (23). In fact, there was an evident link between mTOR
325 and thioredoxin system established. The inhibition of mTOR was found to induce cell
326 death due to the inhibitory effect of TXNIP on the antioxidant pathway (33). By inhibiting
327 mTOR with Torin-1, we observed both reduction in thioredoxin activity and surface thiol
328 density on the NK cells.

329 Another emphasis in the present study would be the importance of antioxidants in relation
330 to immune infiltration and persistence. The thioredoxin system was previously found to
331 explain the persistence of regulatory T cells in the microenvironment with high oxidative
332 stress which could be link to the cell's surface thiol density (5). Similarly, thioredoxin is
333 found to be upregulated in lamina propria T cells as compared to peripheral blood T cells
334 (6). The present study indicates that antioxidants may not just contribute to sustain the
335 killing capacity of NK cells but also equip these NK cells with a bystander role to protect
336 other immune cells within the proximity from ROS-mediated suppression. Given that NK
337 cells residing in the tumor core express higher levels of surface thiol density, these NK

338 cells not only have a reducing barrier to minimize accumulation of intracellular ROS but
339 also possibly to protect other TILs from ROS within the same microenvironment.
340 Moreover, it was demonstrated that the induced production and secretion of thioredoxin
341 in dendritic cells could play a role in T cell activation (26). Even though it was not tested
342 if thioredoxin could be secreted by NK cells, we demonstrated that NK cells with high thiol
343 density could promote infiltration of T cells into autologous tumor spheres. Several studies
344 also demonstrated how “helper” NK cells secrete an array of inflammatory cytokines and
345 chemokines for the homing and priming of other immune cells into the tumor (34-36).
346 Collectively, substantial evidences elucidated how NK cells could turn a “cold” poorly
347 infiltrated tumor into a “hot” inflammatory phenotype that is more compatible for
348 immunotherapy.

349 While current mainstay of adoptive NK cell therapy still utilizes IL-2 in expansion protocols,
350 a number of clinical studies in solid tumors had reported no clinical benefits and low
351 reactivity of these infused NK cells in the tumor (19, 37, 38). The use of IL-15 in adoptive
352 NK cell therapies should be further explored whereby it was observed that endogenous
353 IL-15 production was associated with the persistence of infused NK cells (39). In addition,
354 IL-15 are currently incorporated into multi-specific recombinant protein modalities as next
355 generation antibody-based therapies for cancers (40, 41). In the case of T cell expansion,
356 IL-15 expanded T cells had not only more antioxidant effector molecules but also cytolytic
357 molecules such as granzyme A and granzyme B (42).

358 The study of ROS and its effects on NK cells should also consider the involvement of
359 tobacco smoking - a potent carcinogen with high ROS content (14). Early studies, more
360 than two decades ago found that cigarette smoking decreases NK cells frequency and

361 activity (43, 44). On the other hand, conflicting reports demonstrated that cigarette
362 smoking can stimulate NK cells to produce more IFN γ and other immune effector
363 functions (45, 46). Though the underlying mechanism is not well understood, alveolar
364 macrophages has been proposed to produce ROS to suppresses lung NK cells activity
365 (47). In relation to IL-15, smoking was found to downregulate levels of serum IL-15 levels
366 and its production by activated PBMCs (48, 49). From both our NSCLC cohort and TCGA
367 public database, we observed that tobacco smoking influences the amount of oxidative
368 stress in tumor-infiltrating NK cells and that the expression of intra-tumoral IL-15 could
369 benefit the prognosis of patients that are either current smokers or reformed for less than
370 15 years. Also, by excluding NSCLC patients without any cigarette pack year history of
371 smoking within TCGA, *IL-15* and NK signature score also predicts for favorable survival
372 outcomes (Data not shown). While we did not observe any differences in NK cell gene
373 signature expressed by smokers versus non-smokers (data not shown), it is yet notable
374 that NK cell gene signature score predicts for OS and PFI only in the smoker group.

375 In conclusion, our study exemplify how environmental stress could influence the dynamic
376 TME in cancer. We highlighted the crucial of antioxidants in NK cells and how it can be
377 modulated to improve NK cell-mediated therapies for solid tumors. While IL-15 is already
378 a clinically approved agent, future studies should also explore the implementation of IL-
379 15 into novel cell therapy products for better resistance against oxidative stress. Beyond
380 the application of conventional immune checkpoint inhibitors, the understanding of
381 cellular response to oxidative stress is no doubt required to boost the efficacies of existing
382 immunotherapy treatment regimes.

383 **Materials and Methods**

384 **Cell Culture**

385 The NSCLC cell line H1299 and the chronic myelogenous leukemia cell line K562
386 (American Type Culture Collection (ATCC) were maintained in RPMI medium (Life
387 technology) supplemented with 10% heat-inactivated FBS (Life technology) and 1%
388 antibiotics (penicillin, streptomycin). Patient-derived sarcoma primary cell lines (Case 1,
389 2 and 3 of Table S2) were established from surgical resections and propagated with
390 DMEM medium supplemented with Glutamax (Life technology), 10% heat-inactivated
391 FBS and 1% antibiotics (penicillin, streptomycin).

392 **Tumor Tissue Processing**

393 Tumor resections were processed using Tumor Dissociation Kit (Miltenyi Biotec) and
394 tumor cells were isolated with negative selection-based tumor cells isolation kit (Miltenyi
395 Biotec) according to manufacturer's protocol. For FACS phenotyping, Cell suspensions
396 were washed with FACS buffer (PBS with 5% FBS) and stained for flow cytometry after
397 red blood cell lysis. For TIL proliferation assay, cells were labelled with CFSE (BioLegend)
398 then cultured for 7 days in DMEM/F12 medium supplemented with 10%FBS and 2000
399 IU/ml IL-2 or IL-15 (PeproTech), in the presence or absence of catalase (200 IU/ml,
400 Sigma-Aldrich).

401 **Peripheral Blood Mononuclear Cell, Neutrophils and NK cell isolation**

402 Human peripheral blood mononuclear cells were collected through Ficoll density gradient
403 centrifugation (GE Healthcare). Primary NK cells were isolated by negative selection
404 following the manufacture protocol (Miltenyi Biotec, Human NK cells isolation kit).

405 Neutrophils were enriched from peripheral blood of healthy donors by natural erythrocyte
406 sedimentation method with Dextran (Sigma-Aldrich). Isolated NK cells were cultured in X-
407 vivo 20 medium (Lonza) supplemented with 10% heat-inactivated human AB serum for
408 48 hours, together with 300 IU/ml IL-2 or IL-15 for the cytokine activation. Drugs or vehicle
409 (DMSO) was added on the next day after NK cells were seeded in the plate overnight.
410 Inhibitors used in this study included PX-12 (5 or 10 μ M, SelleckChem), Torin-1 (1 μ M,
411 SelleckChem), N-Ethylmaleimide (2.5mM, Sigma-Aldrich), recombinant thioredoxin-1
412 (5mg/ml, Thermo Fisher). For H₂O₂ treatment, activated NK cells were harvested and
413 washed with PBS twice, then incubated in complete NK medium containing 5 μ M or 10 μ M
414 hydrogen peroxide (Sigma-Aldrich) for 1 hour.

415 For co-culture experiments, autologous neutrophils and NK cells were obtained from fresh
416 peripheral blood of the healthy donor, then seeded into 96 well plate at 6:1 ratio with
417 cytokine support and inhibitor treatment. 1 μ g/ml LPS was added to active neutrophil. Cells
418 were thereafter cultured for 4 days before analyzed by flow cytometry.

419 **TILs expansion**

420 After tumor dissociation, cell suspensions were cultured in AIMV medium (Thermo
421 Scientific) supplemented with 2.5% human AB serum and 3000 IU/ml of IL-15. After 7
422 days, irradiated PBMCs were added at a ratio of 200:1 as feeder cells. Cultures were
423 maintained with 500 IU/ml of IL-15 and functional grade antibody against CD3 (Thermo
424 Scientific) TILs were harvested only after 10 days later for subsequent experiments.

425 **Cytotoxicity assay**

426 Chromium (⁵¹Cr) release assay was used to measure the cytolytic activity of activated
427 NK cells. Briefly, K562 cells were harvested and labelled with ⁵¹Cr (PerkinElmer) as target
428 cells, cytokine activated or sorted NK cells were referred as effector cells. Cells were
429 seeded in 96-well V bottom plate at certain E:T ratio. The supernatants were carefully
430 collected onto LUMA plates (PerkinElmer) after 6- and 16-hours coculture. MicroBeta2
431 (PerkinElmer) was used to detected the radioactivity of the LUMA plate.

432 **Flow Cytometry and Cell Sorting**

433 For surface marker staining, cells were incubated with fluorescence-conjugated
434 antibodies for 20 min at 4°C. For intracellular cytokine staining, NK cells were first
435 stimulated with PMA and ionomycin or cocultured with K562 in the presence of BD
436 GolgiStop™ and GolgiPlug™ for 4h, then subjected to intracellular staining using
437 Cytofix/Cytoperm™ Kit (BD Biosciences). Ki-67 staining was performed with
438 Foxp3/Transcription Factor Staining Buffer Set (eBioscience™). Cytofix/Phosflow Buffer
439 (BD/Biosciences) was used for phosphorylated S6(pS235/pS236) staining. For
440 Intracellular ROS, cells were stained using CellROX™ Deep Red Reagent and measured
441 by flow cytometry following incubating for 30min at 37 °C (Invitrogen™, C10422). Cell
442 viability was analyzed by double staining with AnnexinV and 7-AAD. Cell surface thiol
443 groups were measured by staining with 5uM Alexa Fluor™ 488 C₅ Maleimide (Thermo
444 Fisher, A10254) for 15min on ice. Stained cells were washed twice with FACS buffer then
445 acquired using NovoCyte (ACEA biosciences). FlowJo v10 software (BD) was used to
446 analyze the flow cytometry data. Antibodies used for flow cytometry staining are listed in
447 Table.S3. NK cells were sorted after two days of cytokine stimulation before harvesting
448 and stained with maleimide and Live/Dead cell marker. Using BD FACSAria™ Fusion,

449 NK cells with high and low thiol densities were sorted based on gating of the top and
450 bottom quintiles on maleimide histogram.

451 **Western Blot**

452 NK cells were harvested and lysed in RIPA lysis buffer (Cell Signaling Technology),
453 supplemented with protease and phosphatase inhibitor cocktail (ThermoFisher). The cell
454 lysates were centrifuged at maximum speed for 15min and supernatants were collected.
455 The lysates were boiled for 5 min at 96 °C after adding LDS Sample Buffer and Sample
456 Reducing Agent (NuPAGE, Invitrogen). Proteins were migrated on 4-12% Bis-Tris
457 gradient gels (NuPAGE, Invitrogen) then transferred to PVDF membranes. The
458 membranes were blocked with 5% w/v skim milk before overnight incubation with anti-
459 TXNIP Rabbit mAb (1:1000, Abcam ab188885) at 4 °C. Followed by incubation with anti-
460 rabbit HRP (Abcam, ab6721) for 1 hour at room temperature. Beta-Actin(C4) HRP
461 (SantaCruz-47778) was used after washing the membrane with Restore Western Blot
462 Stripping Buffer (Thermo Fisher) as internal control. Protein bands were developed with
463 Pierce™ ECL Western Blotting Substrate (Thermo Fisher, 32109).

464 **Thioredoxin Activity Assay**

465 Thioredoxin activity of cytokine primed NK cells was measured according to the
466 manufacturer's instruction of the Fluorescent Thioredoxin Assay Kit (FkTRX-02-V2,
467 IMCO). Briefly, 1×10^6 NK cells were lysed in 200 μ l of assay buffer by sonicating. Cell
468 lysates were incubated with thioredoxin reductase and NADPH in the 96-well black micro
469 titer plate at 37 °C for 30 min. Following incubation, fluorescent substrate was added to
470 each sample. The plate was placed in a plate reader (Perkin Elmer Enspire) immediately

471 and fluorescence was recorded at 545nm emission after 520nm excitation for 60 min.
472 Results were calculated and compared in accordance with instructions of the kit.

473 **Sphere formation and infiltration**

474 3D sphere cultures were done with H1299 and 3 patient-derived sarcoma cell lines. For
475 H1299 cell line, 10^4 cells were seeded in Nunclon sphera 96-well Round bottom plate
476 (Thermo Fisher) with complete RPMI medium, single sphere was formed after overnight
477 culture. For sarcoma cell lines, 10^5 cells were seeded in low attachment 12-well plates
478 with DMEM/F12 medium supplemented with 10%FBS and 2.5% Matrigel. Spheres were
479 formed within 3-5 days. Single cells in suspension and cells from loose clusters were
480 removed before the addition of 3×10^5 fluorescent-labelled (either CFSE or CellTrace™
481 Violet) autologous TILs or sorted NK cells. Co-culture of spheres with immune cells were
482 incubated for 48 hours before manual separation and washing of spheres from single cell
483 suspensions. Images of sphere co-cultures were acquired on IncuCyte S3 system (Essen
484 Bioscience, Sartorius). Isolated spheres were then digested with Tumor Dissociation Kit
485 (Miltenyi) to preserve surface markers for FACS analysis. Single cell suspensions of
486 isolated sphere and cells that outside sphere were collected separately for flow cytometry,
487 anti-CD45 antibody was added to identify immune cells and tumor cells.

488 **Confocal Imaging**

489 For mitochondria mass staining, NK cells were incubated with MitoTracker™ Deep Red
490 FM (50nM, Invitrogen™) in FBS free RPMI medium for 30min at 37°C.
491 Foxp3/Transcription Factor Staining Buffer Set (eBioscience) was used to fix and perm
492 cells after the mitochondria staining. Cells were then stained with anti-TXNIP Rabbit mAb
493 (Abcam, ab188885) followed by FITC-conjugated donkey anti-rabbit IgG antibody

494 (BioLegend, #406403). Stained cells were spun onto the slides through cytospin2
495 (SHANDON). Coverslips were mounted on Fluoroshield™ with DAPI histology mounting
496 medium (Sigma-Aldrich). Slide images were acquired with confocal LSM 700 (Zeiss). 40X
497 objective images were processed and analyzed with CellProfiler for TXNIP object counts
498 and fluorescence intensity. 63X objective images were presented as maximum intensity
499 projections as representative images.

500 **RNA isolation and quantitative PCR**

501 RNA was extracted from 5×10^5 cytokine primed NK cells following the manufacture's
502 guidelines of RNeasy Micro Kit (Qiagen). Complementary DNA was synthesized using
503 QuantiTect Reverse Transcription Kit (Qiagen). Quantitative PCR was performed using
504 Power SYBR Green PCR Master Mix (Thermo Fisher). The CFX96 Touch Real-Time
505 PCR Detection System (BioRad) was used to detect SYBR Green incorporation. Relative
506 expressions of target gene were calculated using comparative Ct method and *TBP* was
507 used as an endogenous control. Primer sequences are shown in the Table.S4.

508 **Immunohistochemistry**

509 Fresh tissues were fixed with neutral buffered formalin and embedded in paraffin, then
510 cut into sections following regular histological procedure. After deparaffinization and
511 rehydration, sections were immersed in 10mM sodium citrate buffer (pH 6.0) for heat
512 mediated antigen retrieval. Hydrogen peroxide solution and 4% normal goat serum was
513 used to block endogenous peroxidase and non-specific binding, respectively. The primary
514 antibodies used were anti-NCAM1/CD56 (1:300, Proteintech 14255-1-AP), anti-8-OHdG
515 (1:100, Abcam ab48508). After overnight incubation with primary antibody at 4°C, HRP-
516 conjugated secondary antibody was used for 1 hour at room temperature. 3,3'-

517 diaminobenzidine (DAB) was used as chromogen followed by counterstain with
518 Hematoxylin. Sections were scanned and analyzed via CaseViewer.

519 **Gene expression analysis**

520 The gene expression data were download from GSE77808 (23). Briefly, upon two days
521 of cytokine activation, polysome-associated mRNA that were identified using between IL-
522 2 and IL-15 group using anota as previous described (50). Generally applicable Gene-
523 Set Enrichment was used to identify enrichment of genes with functions annotated by the
524 Gene Ontology Consortium using data for all genes as input. The GSEA analyses were
525 performed using GSEA software (version 4.0.3). The predefined gene sets which
526 representing the comprehensive biological processes are from the Molecular Signatures
527 Database (MSigDB v7.0). We used C5 gene ontology (GO) set for GSEA analysis with
528 cut-off at nominal P-value < 0.01 and the maximum and minimum size for selection were
529 500 and 15 genes, respectively. List of ranked genes are based on NES (normalized
530 enrichment score) which reflects the extent of statistical overrepresentation gene sets in
531 our dataset of differentially expressed genes. Furthermore, to focus on response to
532 reactive oxygen species, gene ontology term GO: 0000302 was used to identify ROS
533 related genes. TBtools was used for heatmap visualization(51).

534 Processed single cell RNA sequencing data was assessed from Gene Expression
535 Omnibus (GEO) database (GSE127465)(52). Using Seqgeq (BD), gene expression was
536 first normalised for dimension reduction by principal component analysis followed by
537 tSNE analysis. NK Cytotoxicity gene set (GZMA, GZMB, GZMH, GZMM, GZMK, PRF1,
538 NKG7, GNLY) was previously defined and used in another study (53). GO pathways from
539 MSigDB database (GO:0051353 and GO:0004791) were imported into the software for

540 enrichment analysis. Enrichment score was calculated by sum of the various gene sets
541 in Seqgeq. The geometric means of enrichment score for defined cell populations were
542 compared and tested for significance in Prism 8 (Graphpad Software).

543 **Processing of TCGA public datasets and gene signature application**

544 Together with normalized gene expression data, raw data for OS and PFI together with
545 “tobacco smoke history” were exported from TCGA public databased accessed from
546 UCSC xena browser (<http://xena.ucsc.edu>). The application of NK cell gene signature for
547 survival analysis (CD160, PRF1, KLRB1, NCR1 and NCR3) was previously used (22, 36).
548 Correlation between two other published NK signatures and *IL15* was done with custom
549 R scripts and package “Corrplot” (54, 55). The oxidative stress gene signature was based
550 on the sum of 42 genes correlated with prognosis in NSCLC dataset previously
551 reported(24). The NSCLC TCGA cohort was then split into two groups based on the
552 patients’ tobacco smoke history before downstream analysis.

553 **Statistics**

554 Using “survival” and survplot R packages, Kaplan-Meier analysis was performed with NK
555 cell signature score or *IL15* gene expression split into a binary (Low/High) variable based
556 on the median value. Both overall survival and progression free interval were used as
557 survival endpoints. Unless stated otherwise, all statistical tests were performed using
558 Prism 8 (Graphpad software). Representation of p-values used *P<0.05, **P<0.01,
559 ***P<0.001, ****P<0.0001 and ns for non-significant.

560

561

562 **Study Approval**

563 This study was approved by the Ethics Committee of the Second Affiliated Hospital of
564 Zhejiang University (IR2019001101) and the Ethical Review Board of Karolinska Institutet
565 (DNR:2013 1979-31). NSCLC surgical resections were collected at the Second Affiliated
566 Hospital of Zhejiang University from 29 patients with primary diagnosis of NSCLC.
567 Sarcoma specimens and matched peripheral blood were obtained at Karolinska
568 University Hospital from 15 sarcoma patients. Written informed consents were signed by
569 all patients before sample acquisition in accordance to the Declaration of Helsinki. The
570 clinicopathologic features of all the cases are shown in Tables S1 and 2.

Author contributions: AL, YY and SYN conceived and designed the project. YY and SYN performed most of the experiments and interpreted the data with the help of ZC, MG, AK and EA. SYN and YC performed the bioinformatic analysis and visualization. WC performed confocal imaging under the supervision of LH. FX provided human sarcoma samples. YW and HX participated in clinical lung cancer sample acquisition under the supervision of KW. YY and SYN composed all figures and wrote the manuscript with key editing by AL and further input from all authors. AL and WK supervised the project and reviewed the manuscript. The order of shared first author was determined by their respective contribution to this project, as YY initiated the project and performed the majority of the experiments; NSY contributed with critical data collection and analysis during later stages and during the revision of the manuscript.

Acknowledgments: We thank Xingyuan Xu, Muye Yang and Zhiqing Fang for technical support. **Funding:** This work was supported by the Swedish Cancer Society (#CAN 2018/451), the Cancer Research Foundations of Radiumhemmet (#181183), The Sagen Foundation and grants from the National Natural Science Foundation of China (Nos. 81902331, 81871874).

571 **References**

- 572 1. Aydin E, Johansson J, Nazir FH, Hellstrand K, and Martner A. Role of NOX2-
573 Derived Reactive Oxygen Species in NK Cell-Mediated Control of Murine
574 Melanoma Metastasis. *Cancer Immunol Res.* 2017;5(9):804-11.
- 575 2. Nakamura K, and Matsunaga K. Susceptibility of natural killer (NK) cells to reactive
576 oxygen species (ROS) and their restoration by the mimics of superoxide dismutase
577 (SOD). *Cancer Biother Radiopharm.* 1998;13(4):275-90.
- 578 3. Stiff A, Trikha P, Mundy-Bosse B, McMichael E, Mace TA, Benner B, et al. Nitric
579 Oxide Production by Myeloid-Derived Suppressor Cells Plays a Role in Impairing
580 Fc Receptor-Mediated Natural Killer Cell Function. *Clin Cancer Res.*
581 2018;24(8):1891-904.
- 582 4. Valko M, Rhodes CJ, Moncol J, Izakovic M, and Mazur M. Free radicals, metals
583 and antioxidants in oxidative stress-induced cancer. *Chemico-biological*
584 *interactions.* 2006;160(1):1-40.
- 585 5. Mougialakos D, Johansson CC, Jitschin R, Bottcher M, and Kiessling R. Increased
586 thioredoxin-1 production in human naturally occurring regulatory T cells confers
587 enhanced tolerance to oxidative stress. *Blood.* 2011;117(3):857-61.
- 588 6. Sido B, Giese T, Autschbach F, Lasitschka F, Braunstein J, and Meuer SC.
589 Potential role of thioredoxin in immune responses in intestinal lamina propria T
590 lymphocytes. *European journal of immunology.* 2005;35(2):408-17.
- 591 7. Collet JF, and Messens J. Structure, function, and mechanism of thioredoxin
592 proteins. *Antioxidants & redox signaling.* 2010;13(8):1205-16.

- 593 8. Holmgren A. Thioredoxin and glutaredoxin systems. *The Journal of biological*
594 *chemistry*. 1989;264(24):13963-6.
- 595 9. Jin R, Gao Y, Zhang S, Teng F, Xu X, Aili A, et al. Trx1/TrxR1 system regulates
596 post-selected DP thymocytes survival by modulating ASK1-JNK/p38 MAPK
597 activities. *Immunology and cell biology*. 2015;93(8):744-52.
- 598 10. Kim SH, Oh J, Choi JY, Jang JY, Kang MW, and Lee CE. Identification of human
599 thioredoxin as a novel IFN-gamma-induced factor: mechanism of induction and its
600 role in cytokine production. *BMC immunology*. 2008;9:64.
- 601 11. Chakraborty P, Chatterjee S, Kesarwani P, Thyagarajan K, Iamsawat S, Dalheim
602 A, et al. Thioredoxin-1 improves the immunometabolic phenotype of antitumor T
603 cells. *The Journal of biological chemistry*. 2019;294(23):9198-212.
- 604 12. Carter BD, Freedman ND, and Jacobs EJ. Smoking and mortality--beyond
605 established causes. *N Engl J Med*. 2015;372(22):2170.
- 606 13. Pfeifer GP, Denissenko MF, Olivier M, Tretyakova N, Hecht SS, and Hainaut P.
607 Tobacco smoke carcinogens, DNA damage and p53 mutations in smoking-
608 associated cancers. *Oncogene*. 2002;21(48):7435-51.
- 609 14. Brody JS, and Spira A. State of the art. Chronic obstructive pulmonary disease,
610 inflammation, and lung cancer. *Proceedings of the American Thoracic Society*.
611 2006;3(6):535-7.
- 612 15. Rizvi NA, Hellmann MD, Snyder A, Kvistborg P, Makarov V, Havel JJ, et al. Cancer
613 immunology. Mutational landscape determines sensitivity to PD-1 blockade in non-
614 small cell lung cancer. *Science*. 2015;348(6230):124-8.

- 615 16. Gettinger S, Choi J, Hastings K, Truini A, Datar I, Sowell R, et al. Impaired HLA
616 Class I Antigen Processing and Presentation as a Mechanism of Acquired
617 Resistance to Immune Checkpoint Inhibitors in Lung Cancer. *Cancer discovery*.
618 2017;7(12):1420-35.
- 619 17. Karre K. Natural killer cell recognition of missing self. *Nat Immunol*. 2008;9(5):477-
620 80.
- 621 18. Vivier E, Tomasello E, Baratin M, Walzer T, and Ugolini S. Functions of natural
622 killer cells. *Nat Immunol*. 2008;9(5):503-10.
- 623 19. Oh S, Lee JH, Kwack K, and Choi SW. Natural Killer Cell Therapy: A New
624 Treatment Paradigm for Solid Tumors. *Cancers*. 2019;11(10).
- 625 20. Lopez-Soto A, Gonzalez S, Smyth MJ, and Galluzzi L. Control of Metastasis by
626 NK Cells. *Cancer Cell*. 2017;32(2):135-54.
- 627 21. Crome SQ, Lang PA, Lang KS, and Ohashi PS. Natural killer cells regulate diverse
628 T cell responses. *Trends Immunol*. 2013;34(7):342-9.
- 629 22. Neo SY, Yang Y, Julien R, Ma R, Chen X, Chen Z, et al. CD73 Immune Checkpoint
630 Defines Regulatory NK-cells within the Tumor Microenvironment. *The Journal of*
631 *clinical investigation*. 2019.
- 632 23. Mao Y, van Hoef V, Zhang X, Wennerberg E, Lorent J, Witt K, et al. IL-15 activates
633 mTOR and primes stress-activated gene expression leading to prolonged
634 antitumor capacity of NK cells. *Blood*. 2016;128(11):1475-89.
- 635 24. Leone A, Roca MS, Ciardiello C, Costantini S, and Budillon A. Oxidative Stress
636 Gene Expression Profile Correlates with Cancer Patient Poor Prognosis:

- 637 Identification of Crucial Pathways Might Select Novel Therapeutic Approaches.
638 *Oxid Med Cell Longev.* 2017;2017:2597581.
- 639 25. Werlenius O, Aurelius J, Hallner A, Akhiani AA, Simpanen M, Martner A, et al.
640 Reactive oxygen species induced by therapeutic CD20 antibodies inhibit natural
641 killer cell-mediated antibody-dependent cellular cytotoxicity against primary CLL
642 cells. *Oncotarget.* 2016;7(22):32046-53.
- 643 26. Angelini G, Gardella S, Ardy M, Ciriolo MR, Filomeni G, Di Trapani G, et al.
644 Antigen-presenting dendritic cells provide the reducing extracellular
645 microenvironment required for T lymphocyte activation. *Proceedings of the*
646 *National Academy of Sciences of the United States of America.* 2002;99(3):1491-
647 6.
- 648 27. Castellani P, Angelini G, Delfino L, Matucci A, and Rubartelli A. The thiol redox
649 state of lymphoid organs is modified by immunization: role of different immune cell
650 populations. *European journal of immunology.* 2008;38(9):2419-25.
- 651 28. Levring TB, Kongsbak-Wismann M, Rode AKO, Al-Jaberi FAH, Lopez DV, Met O,
652 et al. Tumor necrosis factor induces rapid down-regulation of TXNIP in human T
653 cells. *Scientific reports.* 2019;9(1):16725.
- 654 29. Bertini R, Howard OM, Dong HF, Oppenheim JJ, Bizzarri C, Sergi R, et al.
655 Thioredoxin, a redox enzyme released in infection and inflammation, is a unique
656 chemoattractant for neutrophils, monocytes, and T cells. *The Journal of*
657 *experimental medicine.* 1999;189(11):1783-9.

- 658 30. Wagner JA, Rosario M, Romee R, Berrien-Elliott MM, Schneider SE, Leong JW,
659 et al. CD56bright NK cells exhibit potent antitumor responses following IL-15
660 priming. *The Journal of clinical investigation*. 2017;127(11):4042-58.
- 661 31. Mimura K, Kua LF, Shimasaki N, Shiraishi K, Nakajima S, Siang LK, et al.
662 Upregulation of thioredoxin-1 in activated human NK cells confers increased
663 tolerance to oxidative stress. *Cancer immunology, immunotherapy : Cll*.
664 2017;66(5):605-13.
- 665 32. Saxena G, Chen J, and Shalev A. Intracellular shuttling and mitochondrial function
666 of thioredoxin-interacting protein. *The Journal of biological chemistry*.
667 2010;285(6):3997-4005.
- 668 33. Malone CF, Emerson C, Ingraham R, Barbosa W, Guerra S, Yoon H, et al. mTOR
669 and HDAC Inhibitors Converge on the TXNIP/Thioredoxin Pathway to Cause
670 Catastrophic Oxidative Stress and Regression of RAS-Driven Tumors. *Cancer*
671 *discovery*. 2017;7(12):1450-63.
- 672 34. Sedlacek AL, Kinner-Bibeau LB, and Binder RJ. Phenotypically distinct helper NK
673 cells are required for gp96-mediated anti-tumor immunity. *Scientific reports*.
674 2016;6:29889.
- 675 35. Wong JL, Berk E, Edwards RP, and Kalinski P. IL-18-primed helper NK cells
676 collaborate with dendritic cells to promote recruitment of effector CD8+ T cells to
677 the tumor microenvironment. *Cancer Res*. 2013;73(15):4653-62.
- 678 36. Bottcher JP, Bonavita E, Chakravarty P, Blees H, Cabeza-Cabrerizo M,
679 Sammicheli S, et al. NK Cells Stimulate Recruitment of cDC1 into the Tumor

- 680 Microenvironment Promoting Cancer Immune Control. *Cell*. 2018;172(5):1022-37
681 e14.
- 682 37. Bachanova V, Cooley S, Defor TE, Verneris MR, Zhang B, McKenna DH, et al.
683 Clearance of acute myeloid leukemia by haploidentical natural killer cells is
684 improved using IL-2 diphtheria toxin fusion protein. *Blood*. 2014;123(25):3855-63.
- 685 38. Liu E, Tong Y, Dotti G, Shaim H, Savoldo B, Mukherjee M, et al. Cord blood NK
686 cells engineered to express IL-15 and a CD19-targeted CAR show long-term
687 persistence and potent antitumor activity. *Leukemia*. 2018;32(2):520-31.
- 688 39. Miller JS, Soignier Y, Panoskaltsis-Mortari A, McNearney SA, Yun GH, Fautsch
689 SK, et al. Successful adoptive transfer and in vivo expansion of human
690 haploidentical NK cells in patients with cancer. *Blood*. 2005;105(8):3051-7.
- 691 40. Vallera DA, Felices M, McElmurry R, McCullar V, Zhou X, Schmohl JU, et al. IL15
692 Trispecific Killer Engagers (TriKE) Make Natural Killer Cells Specific to CD33+
693 Targets While Also Inducing Persistence, In Vivo Expansion, and Enhanced
694 Function. *Clin Cancer Res*. 2016;22(14):3440-50.
- 695 41. Kim PS, Kwilas AR, Xu W, Alter S, Jeng EK, Wong HC, et al. IL-15 superagonist/IL-
696 15RalphaSushi-Fc fusion complex (IL-15SA/IL-15RalphaSu-Fc; ALT-803)
697 markedly enhances specific subpopulations of NK and memory CD8+ T cells, and
698 mediates potent anti-tumor activity against murine breast and colon carcinomas.
699 *Oncotarget*. 2016;7(13):16130-45.

- 700 42. Kaur N, Naga OS, Norell H, Al-Khami AA, Scheffel MJ, Chakraborty NG, et al. T
701 cells expanded in presence of IL-15 exhibit increased antioxidant capacity and
702 innate effector molecules. *Cytokine*. 2011;55(2):307-17.
- 703 43. Phillips B, Marshall ME, Brown S, and Thompson JS. Effect of smoking on human
704 natural killer cell activity. *Cancer*. 1985;56(12):2789-92.
- 705 44. Tollerud DJ, Clark JW, Brown LM, Neuland CY, Mann DL, Pankiw-Trost LK, et al.
706 Association of cigarette smoking with decreased numbers of circulating natural
707 killer cells. *Am Rev Respir Dis*. 1989;139(1):194-8.
- 708 45. Motz GT, Eppert BL, Wortham BW, Amos-Kroohs RM, Flury JL, Wesselkamper
709 SC, et al. Chronic cigarette smoke exposure primes NK cell activation in a mouse
710 model of chronic obstructive pulmonary disease. *J Immunol*. 2010;184(8):4460-9.
- 711 46. Newman LS, Kreiss K, and Campbell PA. Natural killer cell tumoricidal activity in
712 cigarette smokers and in silicotics. *Clin Immunol Immunopathol*. 1991;60(3):399-
713 411.
- 714 47. Takeuchi M, Nagai S, Nakajima A, Shinya M, Tsukano C, Asada H, et al. Inhibition
715 of lung natural killer cell activity by smoking: the role of alveolar macrophages.
716 *Respiration*. 2001;68(3):262-7.
- 717 48. Mian MF, Pek EA, Mossman KL, Stampfli MR, and Ashkar AA. Exposure to
718 cigarette smoke suppresses IL-15 generation and its regulatory NK cell functions
719 in poly I:C-augmented human PBMCs. *Molecular immunology*. 2009;46(15):3108-
720 16.

- 721 49. Shiels MS, Katki HA, Freedman ND, Purdue MP, Wentzensen N, Trabert B, et al.
722 Cigarette smoking and variations in systemic immune and inflammation markers.
723 *J Natl Cancer Inst.* 2014;106(11).
- 724 50. Larsson O, Sonenberg N, and Nadon R. anota: Analysis of differential translation
725 in genome-wide studies. *Bioinformatics.* 2011;27(10):1440-1.
- 726 51. Chen C, Xia R, Chen H, and He Y. TBtools, a Toolkit for Biologists integrating
727 various HTS-data handling tools with a user-friendly interface. *bioRxiv.* 2018.
- 728 52. Zilionis R, Engblom C, Pfirschke C, Savova V, Zemmour D, Saaticioglu HD, et al.
729 Single-Cell Transcriptomics of Human and Mouse Lung Cancers Reveals
730 Conserved Myeloid Populations across Individuals and Species. *Immunity.*
731 2019;50(5):1317-34 e10.
- 732 53. de Andrade LF, Lu Y, Luoma A, Ito Y, Pan D, Pyrdol JW, et al. Discovery of
733 specialized NK cell populations infiltrating human melanoma metastases. *JCI*
734 *Insight.* 2019;4(23).
- 735 54. Zheng X, Qian Y, Fu B, Jiao D, Jiang Y, Chen P, et al. Mitochondrial fragmentation
736 limits NK cell-based tumor immunosurveillance. *Nat Immunol.* 2019;20(12):1656-
737 67.
- 738 55. Cursons J, Souza-Fonseca-Guimaraes F, Foroutan M, Anderson A, Hollande F,
739 Hedyeh-Zadeh S, et al. A Gene Signature Predicting Natural Killer Cell Infiltration
740 and Improved Survival in Melanoma Patients. *Cancer Immunol Res.*
741 2019;7(7):1162-74.
- 742

Figure 1.

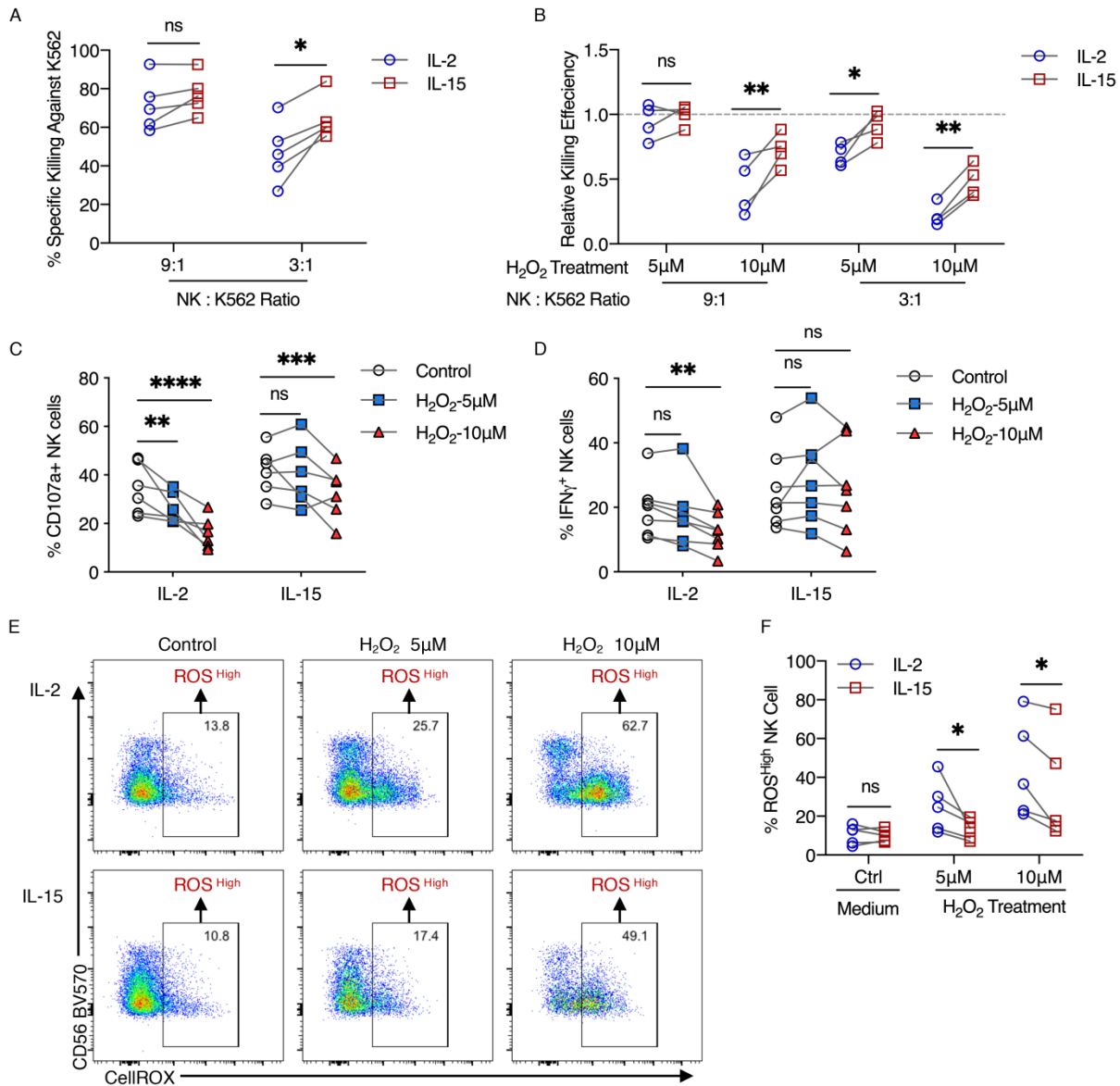


Figure 1. IL-15 primed NK cells mount superior immune response under oxidative stress.

(A) Percentage specific killing of K562 targets by NK cells primed with either IL-2 or IL-15 co-cultured at two different effector to target (E: T) ratios (n=5). (B) Relative killing efficiency at two E:T ratios normalized to control without H₂O₂ treatment for NK cells primed with either IL-2 or IL-15 (n=4). (C) Percentage of CD107a⁺ NK cells primed with either IL-2 or IL-15, in the absence or presence of H₂O₂ treatment. (D) Percentage of IFN γ ⁺ NK cells primed with either IL-2 and IL-15, in the absence or presence of H₂O₂ treatment. (E) Representative panel of FACS plots showing gating strategy of NK cells with high intracellular ROS (n=5). (F) Percentage of IL-15 primed and IL-2 primed NK cells with high intracellular ROS after H₂O₂ treatment (n=5). (A to F) Significance was tested with mixed model analysis with Sidak's multiple comparisons test. *P<0.05, **P<0.01, ***P<0.001 and ****P<0.0001. All individual data points are connected for matching replicates.

Figure 2.

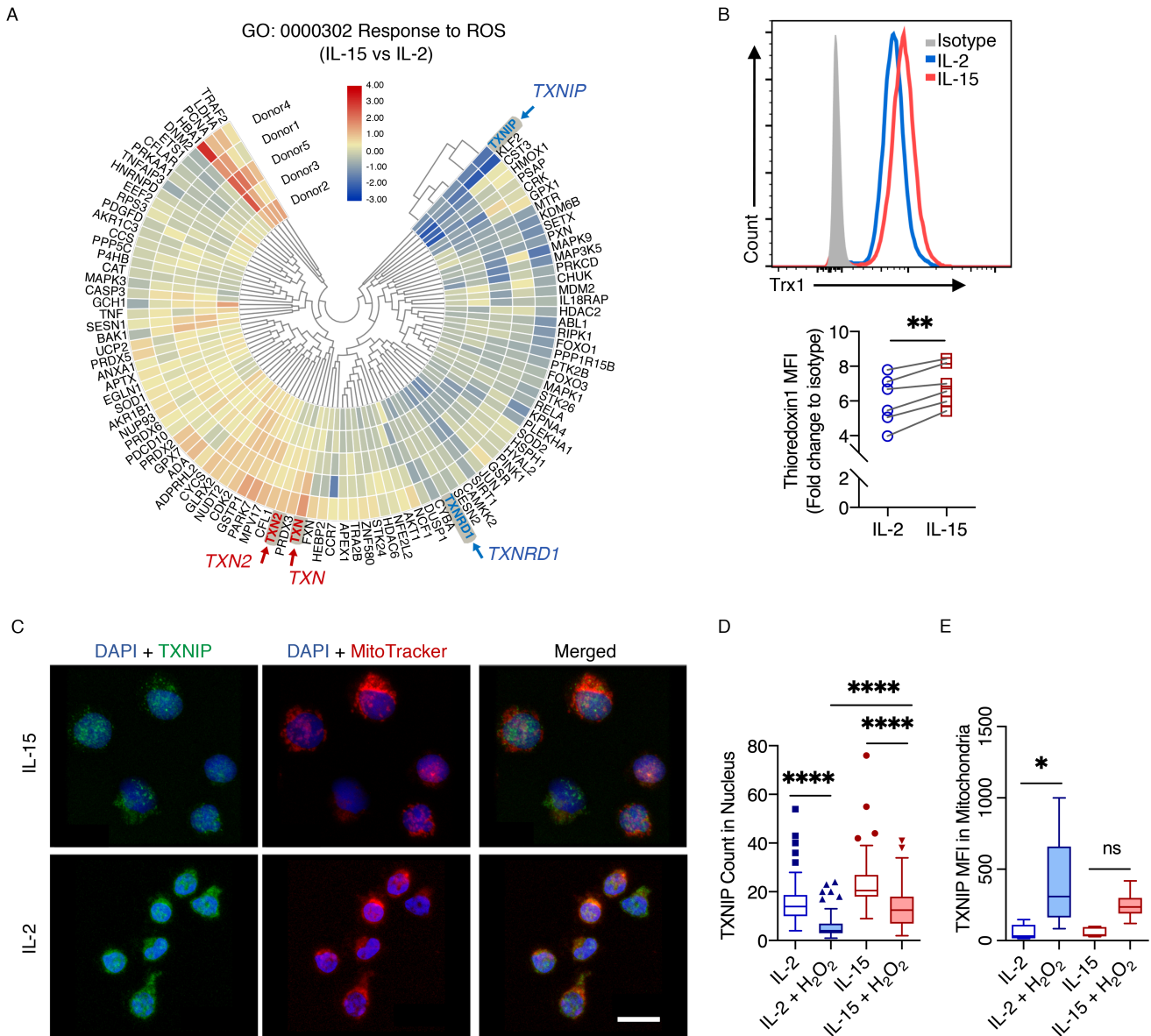


Figure 2. IL-15 upregulates thioredoxin activity in NK cells at both expression levels and reduced shuttling of TXNIP into mitochondria.

(A) Heatmap of differential gene expression in gene ontology (GO:000302) based on IL-15 versus IL-2 primed NK cell comparison. (B) Representative histogram and relative MFI of thioredoxin normalized to isotype control for NK cells. Wilcoxon signed rank test was used to test for significance. (C) Maximum intensity projections of confocal images under 63X objectives for 10 μ M H₂O₂ treated NK cells primed with either IL-15 or IL-2. Blue represents DAPI staining of the nucleus, Green represents TXNIP staining and Red represents mitochondria staining. Scale bar denotes 10 μ m. (D) Image quantification of TXNIP counts (Green objects) per cell nucleus of NK cells with and without treatment of 10mM H₂O₂. (E) Image quantification of TXNIP MFI (Green fluorescent intensity) overlapping with mitochondria (Red objects) of NK cells with and without treatment of 10 μ M H₂O₂. (D and E) Kruskal-Wallis Test was used to test for significance. *P<0.05, **P<0.01 and ****P<0.0001. Data pooled from 3 biological replicates and represented as Tukey boxplots.

Figure 3.

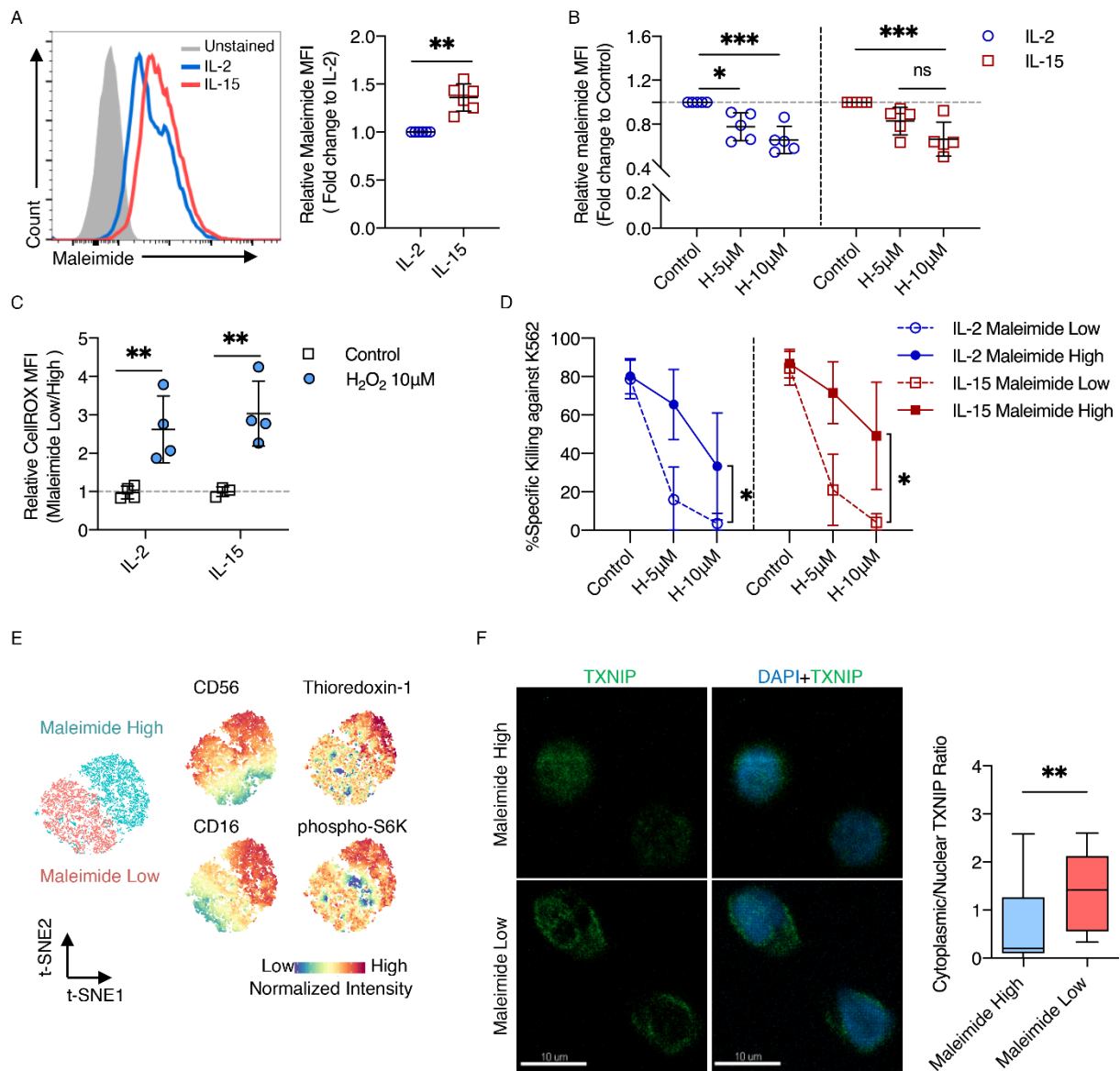


Figure 3. NK cells express surface thiol groups to overcome oxidative stress and sustained cytotoxicity function.

(A) Representative histogram and relative MFI of maleimide staining comparing IL-2 versus IL-15 NK cell cultures (n=6). Significance was tested with Mann-Whitney test. (B) Relative MFI of maleimide staining comparing cells with 1 hour of H₂O₂ treatment in both IL-2 and IL-15 cultures (n=5). (C) Relative MFI of intracellular ROS based on CellIROX staining normalized to maleimide^{low} NK cells (n=4). Ordinary two-way ANOVA with Tukey's test for multiple comparison was used to test for significance. (D) Percentage specific killing of K562 targets at 5:1 effector to target ratio with effector NK cells pre-sorted based on maleimide staining (n=4). (E) T-stochastic neighbor embedding (t-SNE) analysis of NK cells based on surface thiol density (maleimide high vs maleimide low) and its phenotypes acquired by flow cytometry. (F) Representative 63X maximum intensity projection of TXNIP localisation within NK cells sorted by surface density and relative quantification of TXNIP in cytoplasm over nucleus. Green represents TXNIP staining and Blue represents DAPI staining of the nucleus. Scale bar denotes 10µm. Data pooled from 3 biological replicates and represented as Tukey boxplots. Mann Whitney test was used to test for the significance. (B and D) RM two-way ANOVA with Sidak's multiple comparisons test was used to test for significance. All Individual data points are presented as mean ± SD. *P<0.05, **P<0.01 and ***P<0.001.

Figure 4:

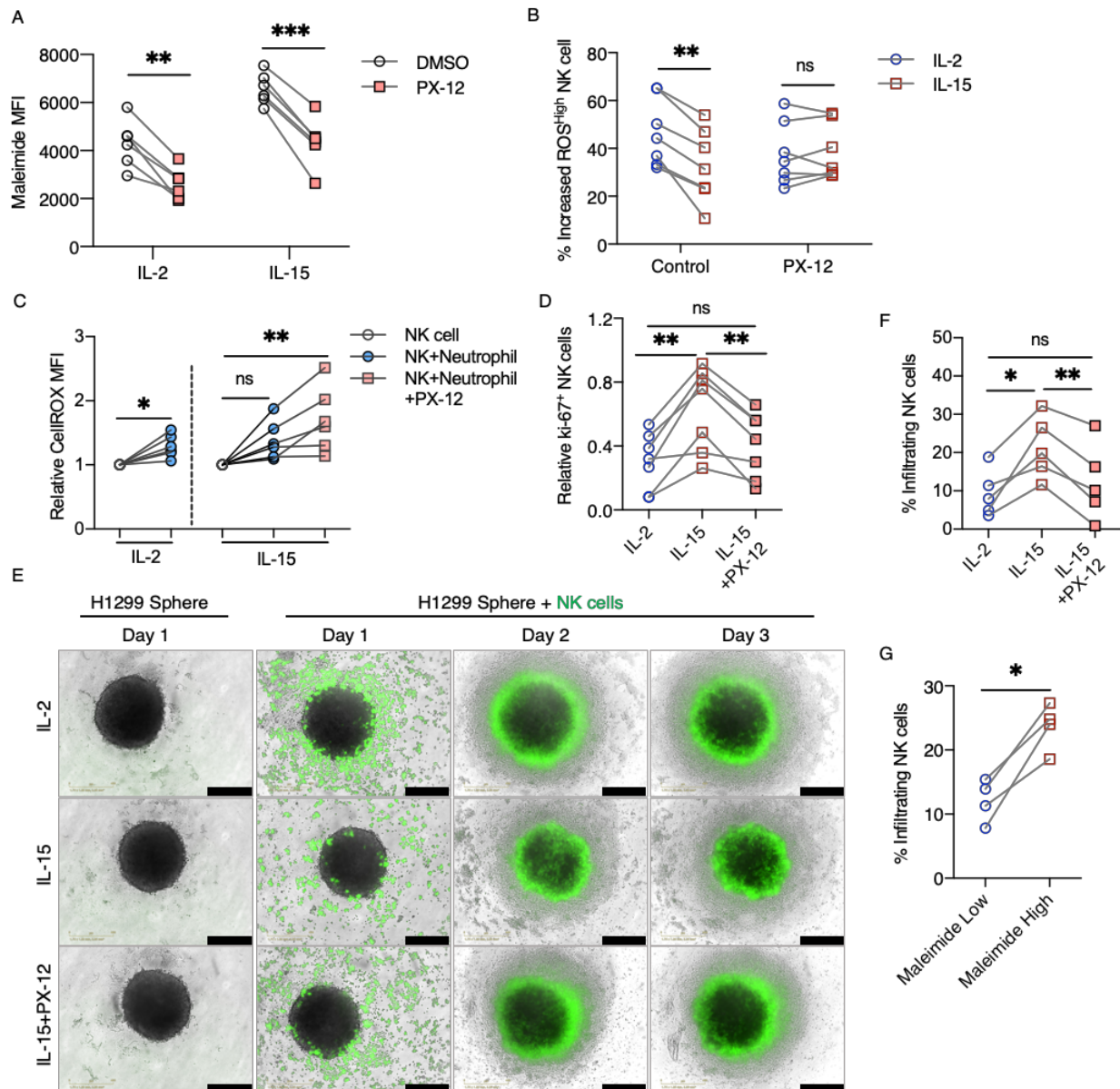


Figure 4. Inhibition of Thioredoxin-1 reduced NK cell surface thiol groups and reversed IL-15 mediated resistance against oxidative stress.

(A) MFI of Maleimide staining on NK cells treated with PX-12 within IL-2 and IL-15 cultures (n=6). **(B)** Percentage of increased ROS^{High} NK cells after 10 μ M H₂O₂ treatment compared to untreated NK cells in the presence or absence of PX-12 within IL-2 and IL-15 cultures (n=6). **(A and B)** RM two-way ANOVA with Sidak's multiple comparisons test was used to test for significance. **(C)** Relative increase in CellROX MFI normalized to control group without neutrophils for NK cell co-cultures and treatment with PX-12 (n=6). Wilcoxon signed rank test was used to test for significance within IL-2 cultures. Friedman test was used to test for significance within IL-15 cultures. **(D)** Relative fold-change in Ki-67 positive NK cells normalized to control group without neutrophils for NK cell co-cultures and treatment with or without PX-12 (n=7). Friedman test was used to test for significance. **(E)** Bright-field images of H1299 tumor spheres with green fluorescence-labelled NK cells acquired under 10X objective at 3 different time points. Bottom right black scale bar denotes 400 μ m. Vertical labels are pre-treatment conditions of NK cells prior to co-culture. **(F)** Percentage of infiltrating NK cells in tumor spheres with different NK cell pre-treatments (n=5). Friedman test was used to test for significance. **(G)** Percentage of infiltrating NK cells in tumor spheres with FACS-sorted NK cells based on maleimide staining (n=4). Paired T-test was performed to test for significance. All individual data points are connected for matching replicates. *P<0.05, **P<0.01, ***P<0.001 and ns for non-significant.

Figure 5.

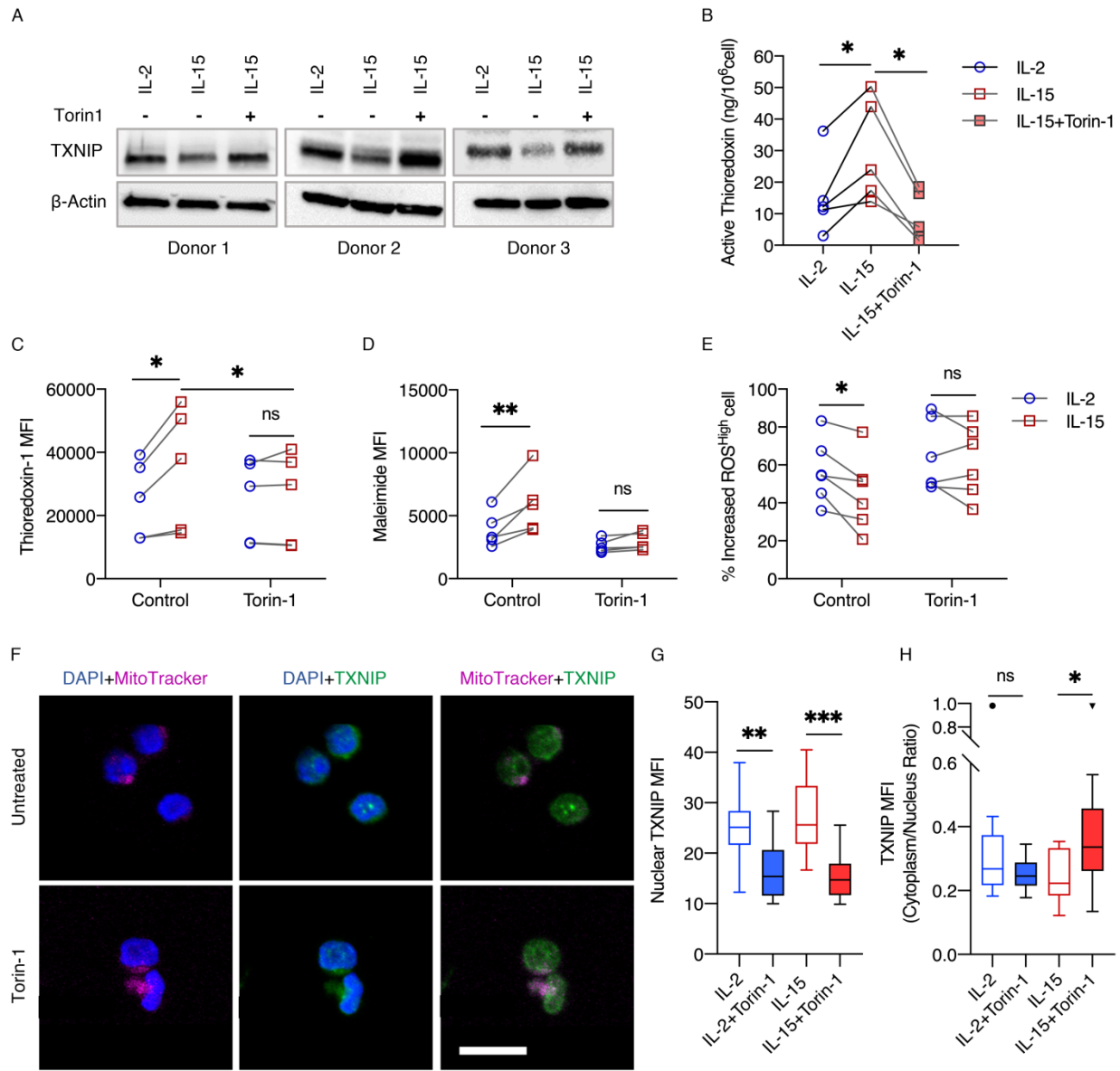


Figure 5. mTOR suppress expression of TXNIP to sustain thioredoxin activity and surface thiol density.

(A) Western blot gel images of TXNIP protein expression in NK cells treated with Torin-1 (n=3). (B) Concentration of active thioredoxin protein in NK cells primed with either IL-2 or IL-15 and IL-15 treated with Torin-1 (n=5). Friedman test was used to test for significance. (C) MFI of Thioredoxin-1 expressed in NK cells primed with either IL-2 or IL-15 and treatment with Torin-1 (n=5). (D) MFI of maleimide staining on NK cells primed with either IL-2 or IL-15 and treatment with Torin-1 (n=5). (E) Relative increased percentage of ROS^{High} NK cells compared to without H₂O₂ for NK cells primed with either IL-2 or IL-15 and treatment with Torin-1 after 10μM H₂O₂ exposure (n=6). (F) Representative maximum intensity projections of confocal images under 63X objectives for 1mM Torin-1 treated NK cells. Blue represents DAPI staining of the nucleus, Green represents TXNIP staining and Magenta represents mitochondria staining. Scale bar denotes 10μm. (G) MFI of TXNIP (Green fluorescent intensity) within nuclear area of NK cells under H₂O₂ oxidative stress. (H) Image quantification of Cytoplasm: Nucleus ratio of TXNIP MFI on NK cells under H₂O₂ oxidative stress. (C-E) RM two-way ANOVA with Sidak's multiple comparisons test was used to test for significance. All individual data points are connected for matching replicates. (G and H) Kruskal-Wallis Test was used to test for significance. *P<0.05, **P<0.01 and ****P<0.0001. Data pooled from 3 biological replicates and represented as Tukey boxplots. *P<0.05, **P<0.01 and ns for non-significant.

Figure 6.

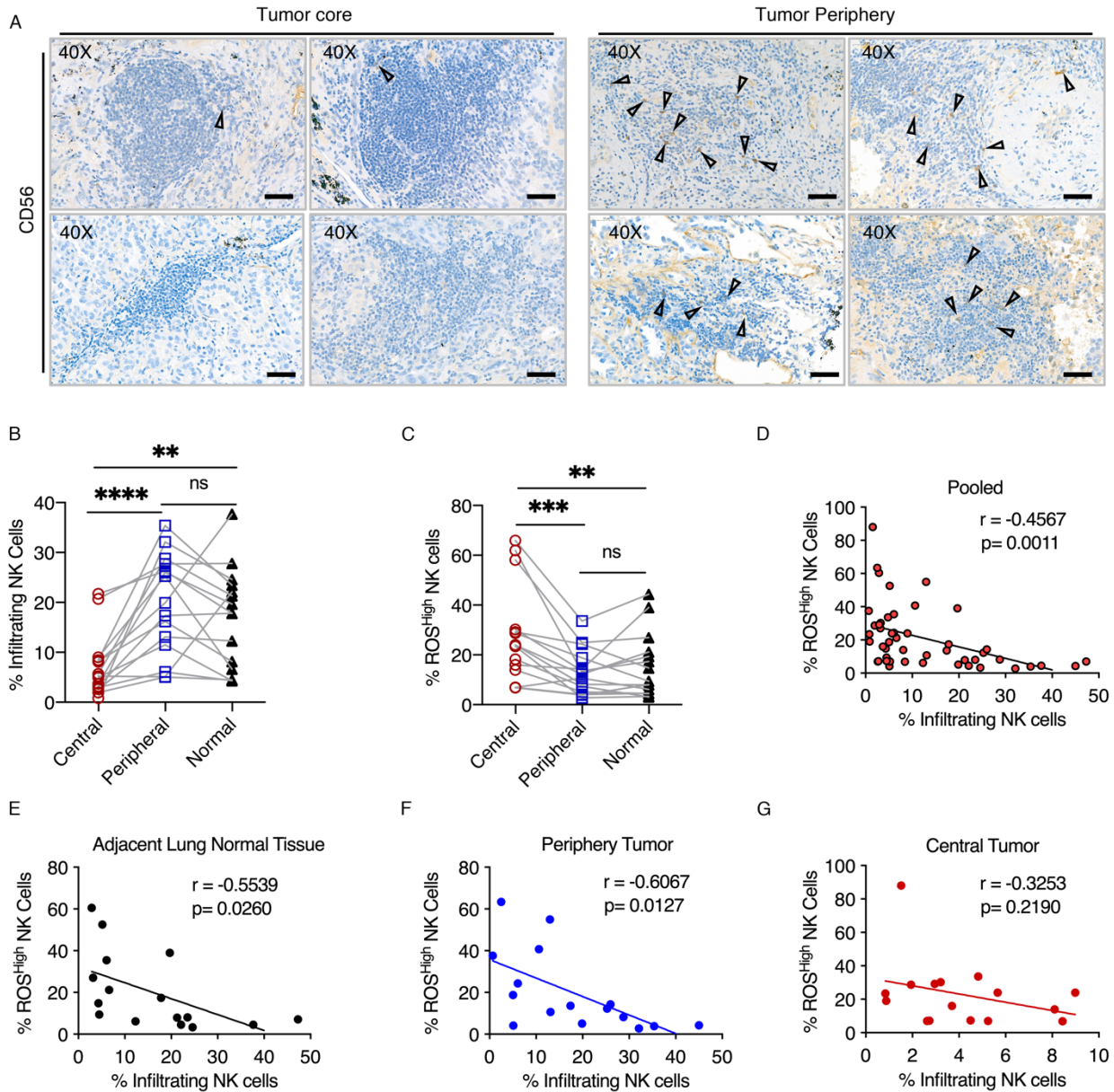


Figure 6. NK cell infiltration is influenced by the accumulation of oxidative stress in NSCLC tumors.

(A) Representative images of immunohistochemistry (IHC) staining of CD56 within immune infiltrates found in NSCLC tumor core and tumor periphery under 40X magnification. The triangles indicate CD56 positive lymphocytes. Scale bar denotes 50 μ m(n=4). **(B)** Percentage of infiltrating NK cells in different patient tissues collected (n=16). **(C)** Percentage of ROS^{High} NK cells in different patient tissues collected (n=16). **(D-G)** Correlation of ROS^{High} NK cells over percentage of infiltrating NK cells isolated in **(D)** pooled tissue samples (n=48), **(E)** adjacent lung normal tissue (n=16), **(F)** Periphery tumor(n=16) and **(G)** Central tumor (n=16). Spearman's rank correlation coefficient was done to test for significant correlation. **(B and C)** All matching data points for autologous samples are connected with lines. Friedman Test was used to test for significance. **P<0.01, ****P<0.001 and ns for non-significant.

Figure 7.

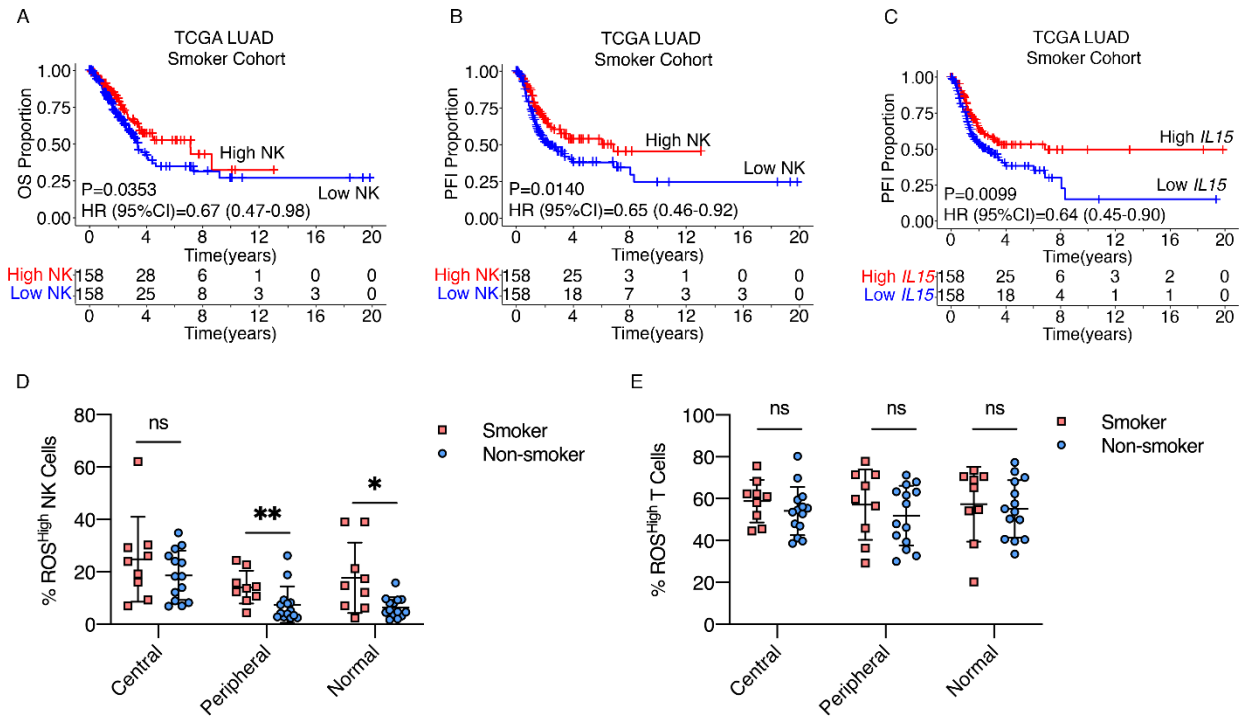


Figure 7. NK cell signature and *IL15* gene expression predict for better prognosis in NSCLC patients with smoking history.

(A) Overall survival (OS) of TCGA-NSCLC smoker cohort based on median of NK gene signature score. **(B)** Progression Free Interval (PFI) of TCGA-NSCLC smoker cohort based on median of NK gene signature score. **(C)** PFI of TCGA-NSCLC smoker cohort based on median of *IL15* gene expression. **(A-C)** Logrank test was used to test for significance in differences in survival distribution ($n=316$). **(D)** Percentage of ROS^{High} NK cells in different patient tissues classified by patient's smoking history. **(E)** Percentage of ROS^{High} T cells in different patient tissues classified by patient's smoking history. **(D and E)** All Individual data points presented with mean \pm SD. ($n=9$ smokers and 14 non-smokers). Ordinary two-way ANOVA with Sidak's multiple comparisons test was used to test for significance.

Figure 8.

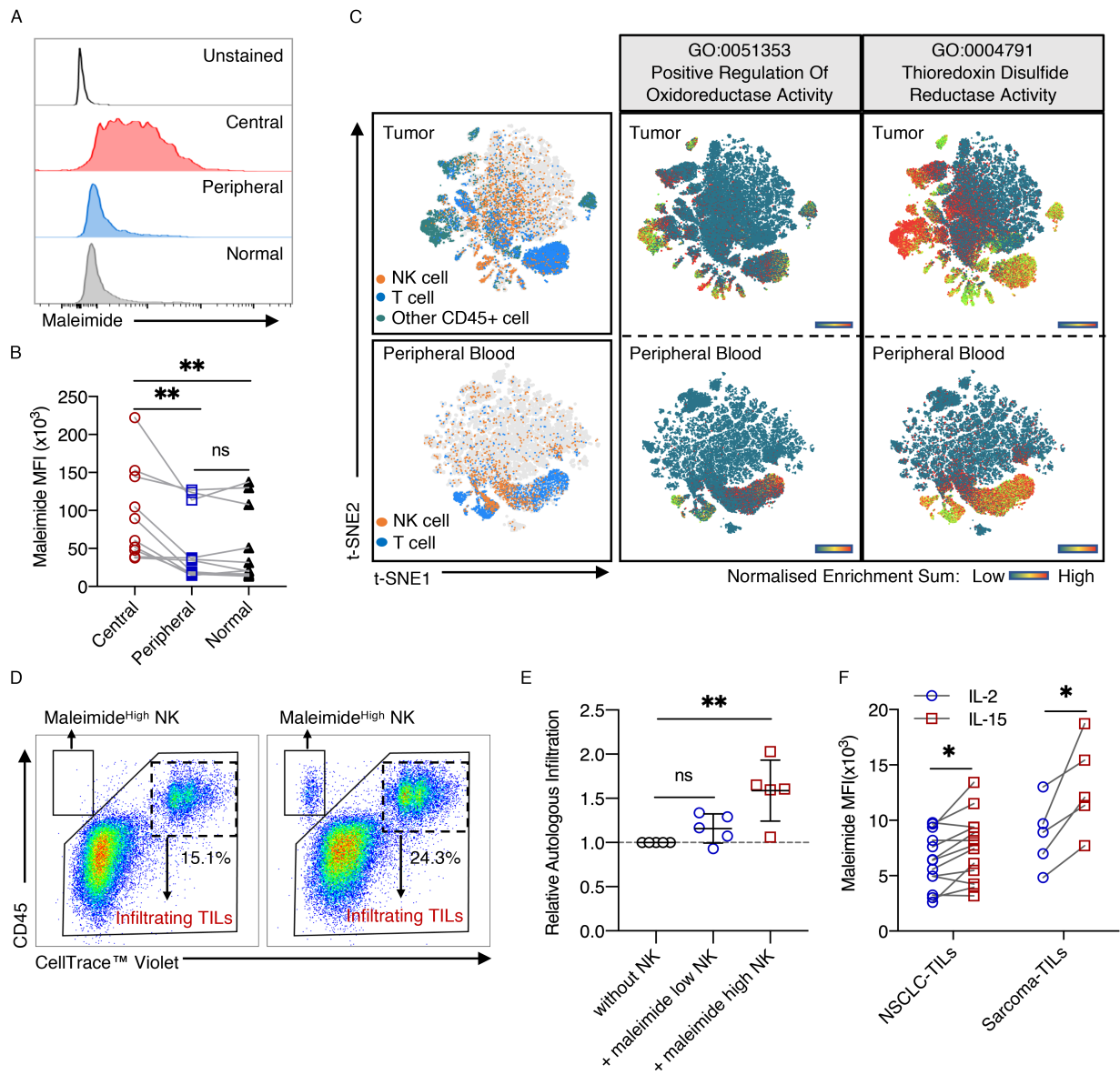


Figure 8. High surface thiol densities on tumor infiltrating NK cells improve immune infiltration into tumors.

(A) One of ten representative histogram of maleimide staining on gated NK cells in different types of tissue samples isolated from NSCLC patients. **(B)** MFI of maleimide staining comparing NK cells residing in different types of tissue samples from NSCLC patients. Matched individual data points are connected with lines (n=10). Friedman test was used to test for significance. **(C)** t-distributed stochastic neighbor embedding (tSNE) projections of single cell RNA analysis from pooled NSCLC tumors (n=7) and patients' peripheral blood (n=6). Heatmap scale represents the normalized enrichment sum for GO:0051353 and GO:0004791. **(D)** Representative FACS plots showing gating strategy for analysis of autologous TILs infiltration into tumor sphere (n=5). **(E)** Relative ratio of percentage autologous infiltration normalized to "without NK" control (n=5). All data points presented with mean \pm SD. Kruskal-wallis with Dunn's multiple comparison test was used to test for significance. **(F)** MFI of maleimide staining of NK cells in TILs expansion comparing IL-2 primed and IL-15 primed cultures after 7 days (n= 5 sarcoma and 13 NSCLC). Matched individual data points are connected with lines. Significance was tested with mixed model analysis with Sidak's multiple comparisons test. All matching replicates were connected by lines. *P<0.05 and **P<0.01.